Probing the Biomechanical Contribution of the Endothelium to Lymphocyte Migration: Diapedesis by the Path of Least Resistance.

Roberta Martinelli[1,2], Adam S. Zeiger[3], Matthew Whitfield[3], Tracey E. Scuito[4], Ann Dvorak[4], Krystyn J. Van Vliet[3,5], John Greenwood[2,‡] and Christopher V. Carman[1,‡]

Supplemental Figure Legends

Fig. S1. Assessing parameters of total lymphocyte migration, adhesion, endothelial cell geometry and adhesion molecule expression. (**a**) Schematic of stages of diapedesis. **(b)** 'Total Diapedesis'. Primary rat brain (rB), rat heart (rH), human lung (hL) and heart (hH) MVECs were grown to confluence and stimulated with TNF-α (24 h) before addition of rat or human T cells for 10 min (black bars; all ECs) or 30 min (white bars; rB only) to perform migration experiments. Samples were fixed, permeabilized, stained and quantified as described in *Material and Methods*. Data are the mean ± SEM of at least three separate experiments. (**c**) Cell area and junctional perimeter of primary rat brain (rB) and rat heart (rH) where calculated by manually tracing every cell in each field with the Axiovision software. Measurements were made for least three fields per cell type (cell n>15). (**d**) Primary rat brain and (**e**) rat heart MVECs were grown to confluence, stimulated with TNF-α (24 h) and treated with Adrenomedullin (AM, 10 μM) and 8-pCPT-2'O-Me-cAMP (O-Me, 200 μM) for 30 min and Histamine (His, 300 μM) and PP2 (10 μM) for 10 min prior to addition of T cells for adhesion or diapedesis experiments or (**f**) staining for surface expression of ICAM-1,

VCAM-1 and PECAM-1 and flow cytometric analysis. Data are the mean ± SEM of at least three separate experiments.

Fig. S2. Modulation of junctional integrity in hLMVECs and effects on diapedesis. hLMVECS were grown to confluence and stimulated with TNF-α (24 h) before addition of Adrenomedullin (AM, 10 μM), 8-pCPT-2'O-Me-cAMP (O-Me, 200 μM), Histamine (His, 300 μM) and PP2 (10 μM). (**a, b**) Human T cells were added for 10 min prior to adhesion or diapedesis experiments. (**c**) Changes in TEER are shown following treatments. Data are the mean ± SEM of at least four separate experiments. (**d**) Immunofluorescence imaging of hLMVECs following treatment with AM and O-Me for 30 min and His or PP2 for 10 min prior to fixation, permeabilization, staining for VEC (green) and F-Actin (red) (i) and quantitation of number of gaps per field (ii) and % of total gap area per field (iii) in PP2 and His treated cells. White arrowheads, cortical actin; yellow arrowheads, gaps. Scale Bars, 10 μm. Data are representative of at least five separate experiments. **(e)** hLMVEC were treated as above prior to addition of human T cells for 10 min followed by fixation, staining and quantitation for transcellular (i) and paracellular diapedesis (ii). Data are the mean ± SEM of at least four separate experiments.

Fig. S3. Assessing expression and distribution of adhesion molecules on hLMVEC following treatment with barrier-altering agents. (**a**) hLMVEC were grown to confluence and stimulated with TNF-α (24 h) before treatment with Adrenomedullin (AM, 10 μM) and 8-pCPT-2'O-Me-cAMP (O-Me, 200 μM) for 30 min and Histamine (His,

300 μM) and PP2 (10 μM) for 10 min prior to staining for surface expression of ICAM-1, VCAM-1 and PECAM-1 and flow cytometric analysis. (**b**) hLMVECs were grown to confluence and stimulated with TNF-α (24 h) prior to treatment as in (a). Cells were fixed and stained for ICAM-1, VCAM-1 and VEC or PECAM-1 and analysed by confocal microscopy. White lines indicate the area used for intensity analysis, which is shown in the corresponding line graphs below each image. Scale Bars, 10 μm. Data are representative of at least three different experiments.

Fig. S4. Characterization of fluid shear effects, fluorescence permeability assay, EC responses to substrate stiffness, ILP probing and Cytochalasin D treatment. **(a)** hLMVEC were grown to confluence, stimulated with TNF-α (24 h) and exposed to short or long shear (30 min or >36 h, respectively 10 dyne/cm^2). Shear was stopped and cells were fixed and stained for actin 10 min after shear cessation. Scale Bars, 10 μm (i). hLMVEC were shear pre-conditioned as in (i) and human T were added for 10 min under static condition then fixed, stained and imaged to quantify total diapedesis (ii). Data are the mean ± SEM of at least four separate experiments. **(b)** Endothelial permeability following treatment with Adrenomedullin (AM, 10 μM) or Histamine (His, 300 μM) was measured with a fluorescently based assay. Cells were fixed and imaged (i) and quantitation was performed as described in Materials and Methods (ii). **(c)** Human lung MVEC were grown to confluence either on glass (>10 GPa) or on elastic surfaces of 28 kPa and 1.5 kPa, stimulated with TNF-α (24 h) before fixation and staining for F-actin. **(d)** Live-cell imaging of T cell ILP probing on hLMVECs (i) or primary rat Brain MVEC (ii) that were grown to confluence, stimulated with TNF-α (24

h), stained with memR18 (to mark the plasma membrane). DIC (upper panels) and membrane fluorescence (lower panels) are shown. Note formation and disapperance of multiple fluorescent rings (i.e., 'podo-prints'; red arrows) reflective of T cell ILP formation. A transcellular pore (dashed yellow line) is shown in hLMVEC. Images are representative of at least four separate experiments. Scale Bars, 2 μm. **(e)** hLMVEC transfected with actin-GFP were grown to confluence, stimulated with TNF-α (24 h) and left untreated or treated with cytochalasin D (200nM, 30 min at 37ºC). Note the complete depletion of actin filaments throughout the cell body with maintenance of cortical actin at the inter-endothelial junctions. The images are representative of at least 7 separate experiments. Scale Bars, 10 μm.

Supplemental Movie Legends

Movie 1: Lymphocytes palpate the endothelium through invadosome-like protrusions (ILPs). Live-cell imaging of lymphocyte lateral migrating on MVEC transfected with memDsRed (magenta) and cytoplasmic-YFP (green). Parts I and II show a lymphocyte probing the endothelial cell junction or the cell body, respectively. Note the dynamic appearance and disappearance of circular rings of memDsRed fluorescence that correspond to cell surface invaginations ('podo-prints') reflective of invadosome-like protrusions (ILP) that are devoid of cytoplasmic-YFP. Images were acquired by time-lapse microscopy (Axiovert 200M; Carl Zeiss). Frames were taken every 30 s. See corresponding Fig.5c.

Movie 2: Frustrated ILPs probing on top of the nucleus. Live-cell imaging of a lymphocyte laterally migrating on MVEC transfected with mem-YFP (green). Note

appearance of multiple ‘non-productive/frustrated’ podo-prints/ILP probing on top of the nucleus, followed by appearance of ILP and a transcellular breach point immediately adjacent to the nucleus. Images were acquired by time-lapse microscopy (Axiovert 200M; Carl Zeiss). Frames were taken every 30 s. See corresponding Fig.7b.

Movie 3: Lateral T cell migration and ILP probing across endothelial junctions without diapedesis. Live-cell imaging of lymphocytes laterally migrating on MVEC transfected with memDsRed (magenta) and actin-GFP (green). Note three separate lymphocytes migrating laterally and avidly probing over a junction, without initiating a diapedesis event. Images were acquired by time-lapse microscopy (Axiovert 200M; Carl Zeiss). Frames were taken every 30 s.

Movie 4: Frustrated ILPs probing and failed diapedesis in zones of dense F-actin. Live-cell imaging of lymphocytes laterally migrating on MVEC transfected with memDsRed (magenta) and actin-GFP (green). Note the frustrated and prolonged probing of a lymphocyte in an actin-dense area (lower left) without breaching of the endothelium. Another lymphocyte succeeds in creating a transcellular pore, but it is unable to sufficiently deform the actin meshwork to allow for migration, resulting in a failed diapedesis attempt. Images were acquired by time-lapse microscopy (Axiovert 200M; Carl Zeiss). Frames were taken every 30 s. See corresponding Fig.8ai.

Movie 5: Avid ILP-mediated distortion of F-actin networks during lateral migration and ultimate diapedesis. Live-cell imaging of a lymphocyte laterally migrating on MVEC transfected with memDsRed (magenta) and actin-GFP (green). Note that in the zone of

modest F-actin density ILP probing causes appreciable bending and distortion of endothelial actin filaments, coupled to successful breaching of (and diapedesis across) the endothelium, when a zone of relatively reduced density of actin was reached. Images were acquired by time-lapse microscopy (Axiovert 200M; Carl Zeiss). Frames were taken every 30 s. See corresponding Fig.8b.

Movie 6: ILP-mediated endothelial cell breaching between two actin fiber to initiate diapedesis. Live-cell imaging of a lymphocyte laterally migrating on MVEC transfected with memDsRed (magenta) and actin-GFP (green). Note that the lymphocyte in a low F-actin density zone readily breaches and migrates across the endothelium by extending ILP between two actin filaments, which subsequently are 'bowed out' and distorted to accommodate completion of diapedesis. Images were acquired by time-lapse microscopy (Axiovert 200M; Carl Zeiss). Frames were taken every 30 s. See corresponding Fig.8aii.

Movie 7: Depletion of F-actin promotes avid transcellular diapedesis. Live-cell imaging of lymphocytes laterally migrating on MVEC that were transfected with memDsRed (magenta) and actin-GFP (green) and pre-treated with Cytochalasin D (200nM, 30 min) to deplete actin filaments. Note that actin filaments were profoundly lost within the endothelial cell body while a dense cortical actin ring was maintained at the junctions. In these conditions an extensive number of transcellular events can be seen, including several particular that were extremely close, but not migrating through the intact junction. See corresponding figure (Fig 8d) for post-fixation staining of VEC. Images

were acquired by time-lapse microscopy (Axiovert 200M; Carl Zeiss). Frames were taken every 20 s.

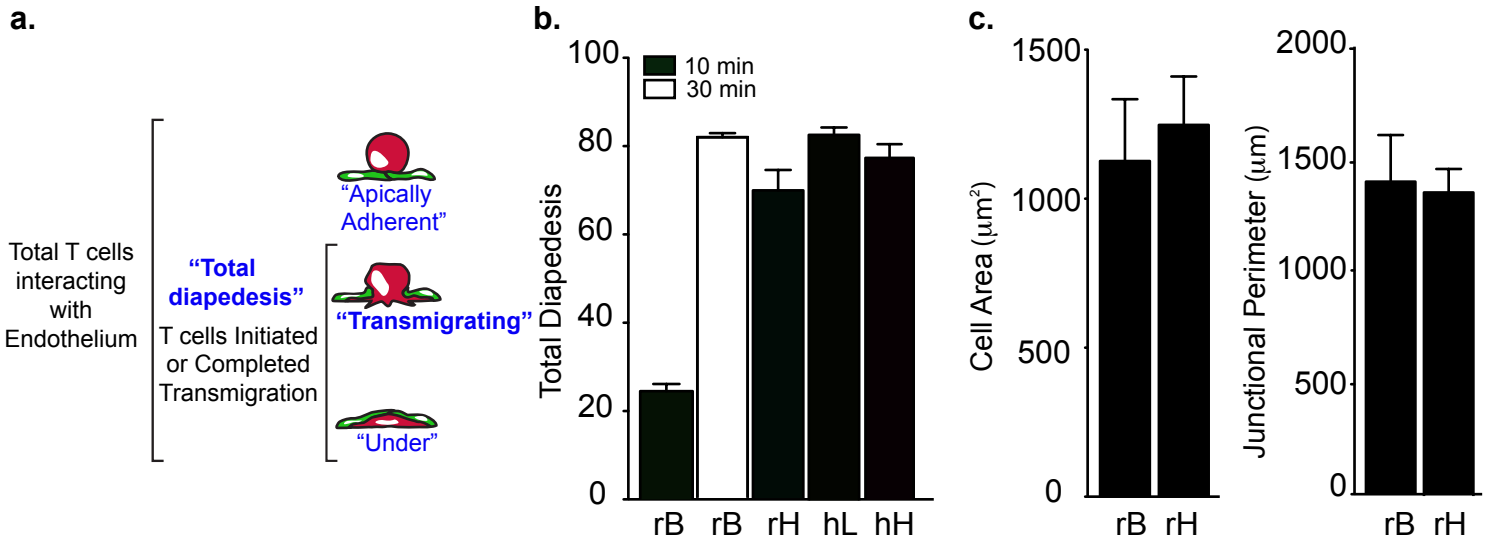
a.
Total T cells interacting with Endothelium
"Total diapedesis"
T cells Initiated or Completed Transmigration
"Apically Adherent"
"Transmigrating"
"Under"
b.
10 min
30 min
Total Diapedesis
rB rB rH hL hH
c.
Cell Area (μm²)
rB rH
Junctional Perimeter (μm)
rB rH

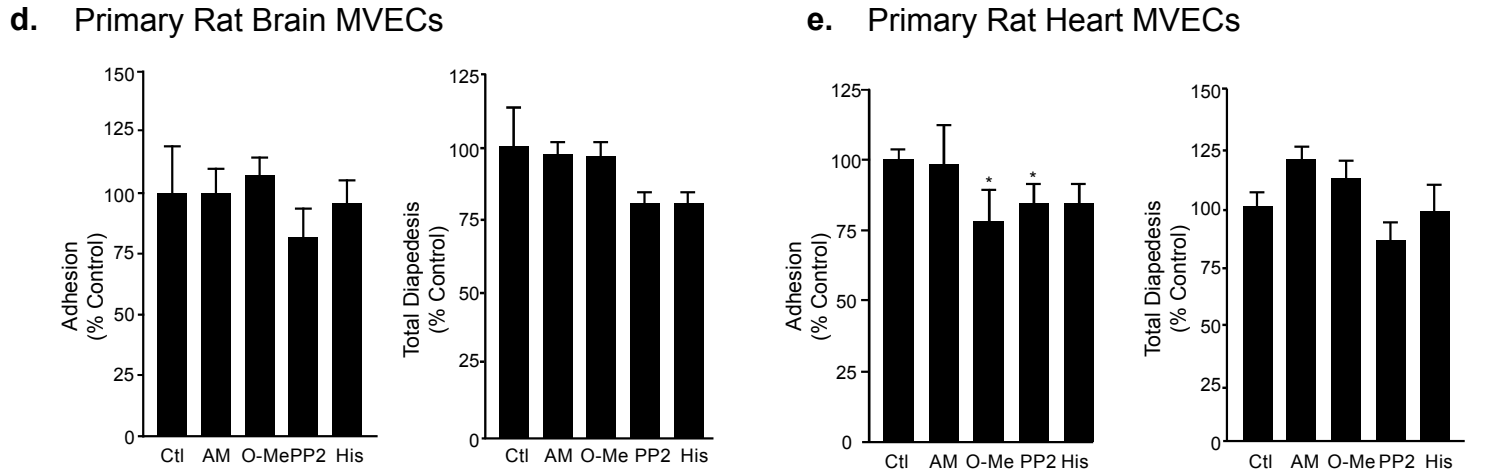
d. Primary Rat Brain MVECs
Adhesion (% Control)
Total Diapedesis (% Control)
Ctl AM O-Me PP2 His
e. Primary Rat Heart MVECs
Adhesion (% Control)
Total Diapedesis (% Control)
Ctl AM O-Me PP2 His

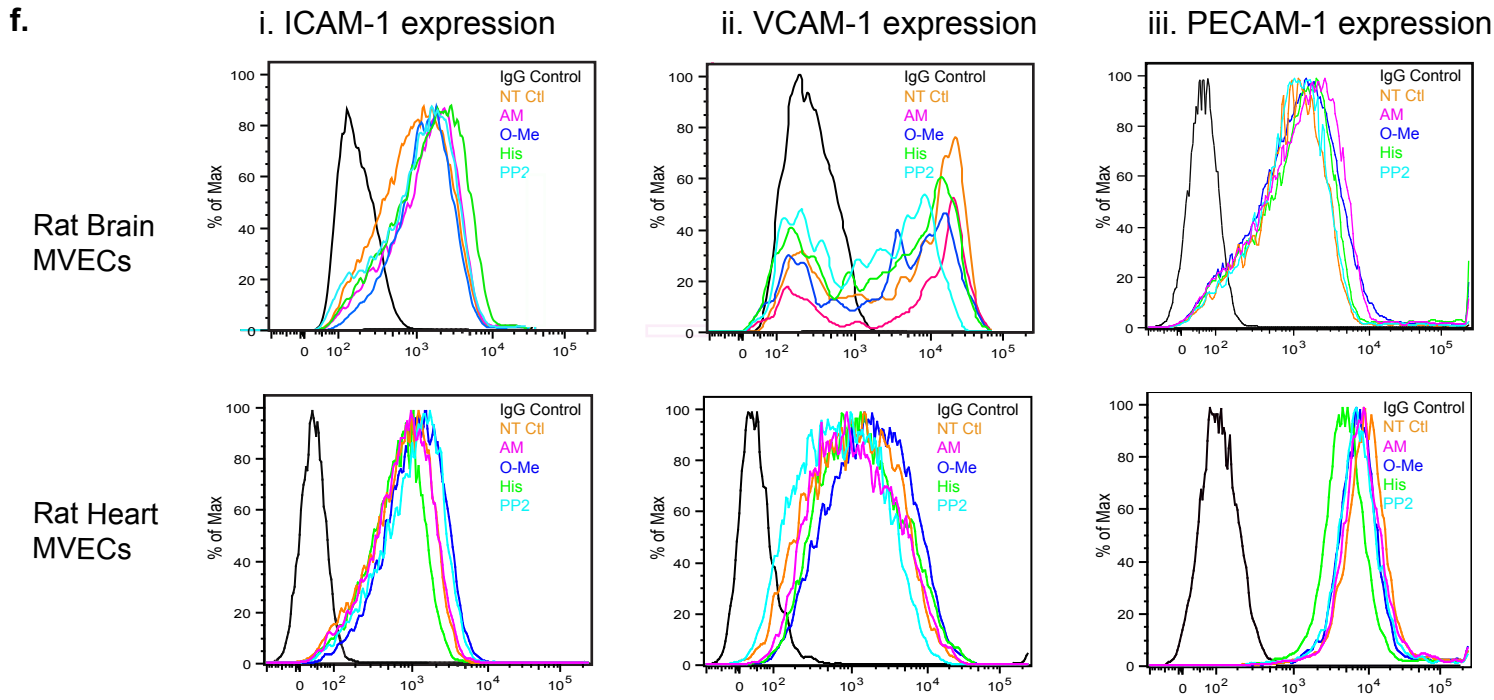
f.
i. ICAM-1 expression
ii. VCAM-1 expression
iii. PECAM-1 expression
Rat Brain MVECs
Rat Heart MVECs
% of Max
IgG Control
NT Ctl
AM
O-Me
His
PP2

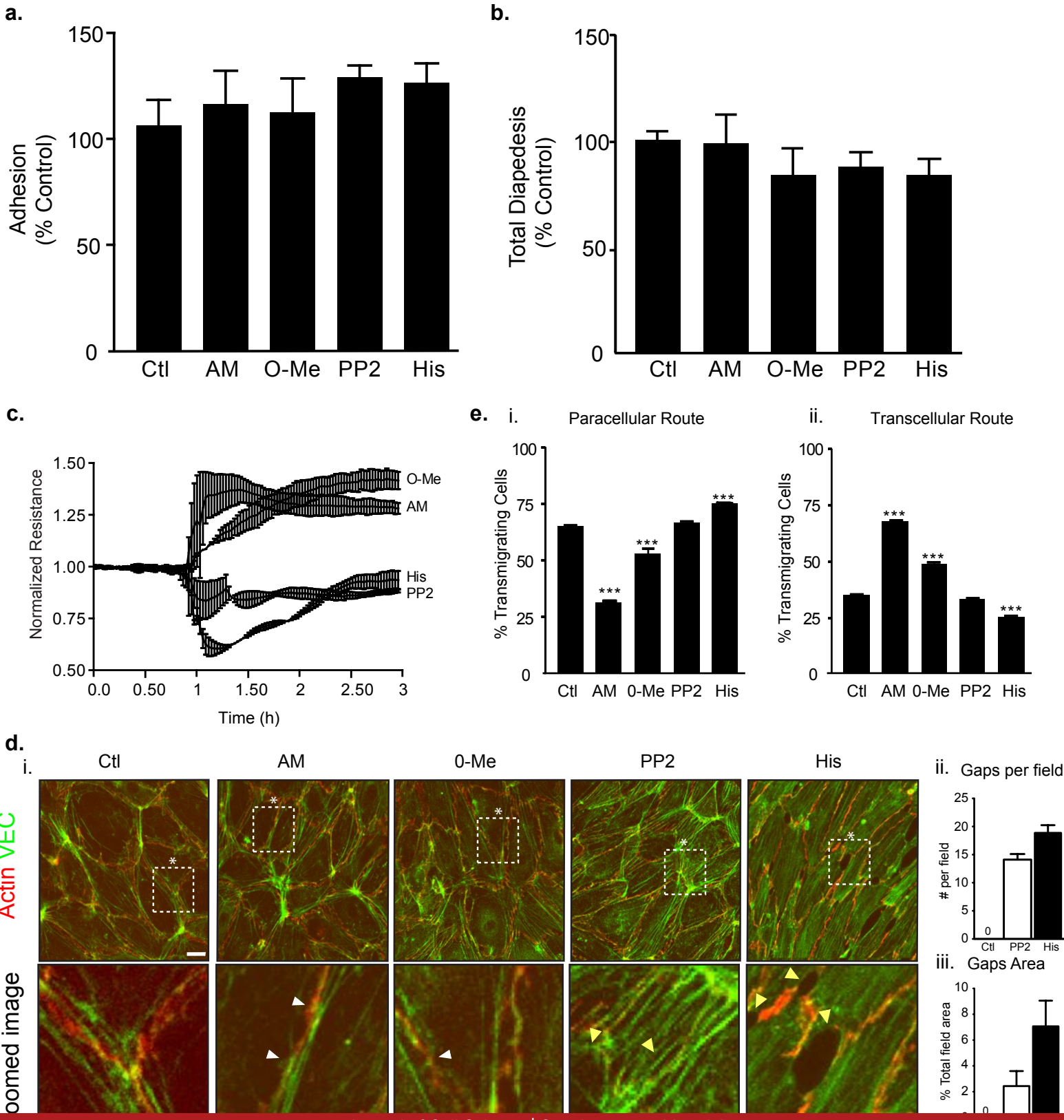
a.
Adhesion (% Control)
150
100
50
0
Ctl
AM
O-Me
PP2
His
b.
Total Diapedesis (% Control)
150
100
50
0
Ctl
AM
O-Me
PP2
His
c.
Normalized Resistance
1.50
1.25
1.00
0.75
0.50
0.0
0.50
1
1.50
2
2.50
3
Time (h)
O-Me
AM
His
PP2
e.
i.
Paracellular Route
% Transmigrating Cells
100
75
50
25
0
***
Ctl
AM
0-Me
PP2
His
ii.
Transcellular Route
% Transmigrating Cells
d.
i.
Ctl
AM
0-Me
PP2
His
Actin VEC
oomed image
ii.
Gaps per field
per field
25
20
15
10
5
0
Ctl
PP2
His
iii.
Gaps Area
% Total field area
10
8
6
4
2
0

a.

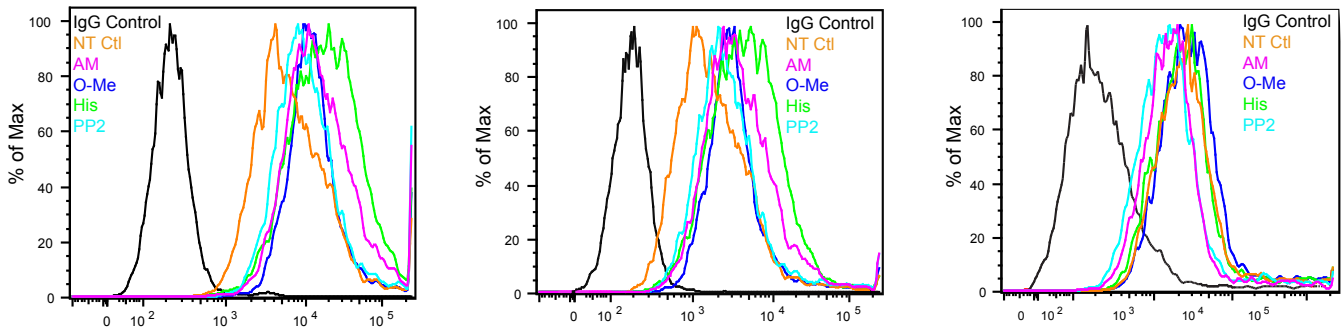
IgG Control
NT Ctl
AM
O-Me
His
PP2
% of Max

b.

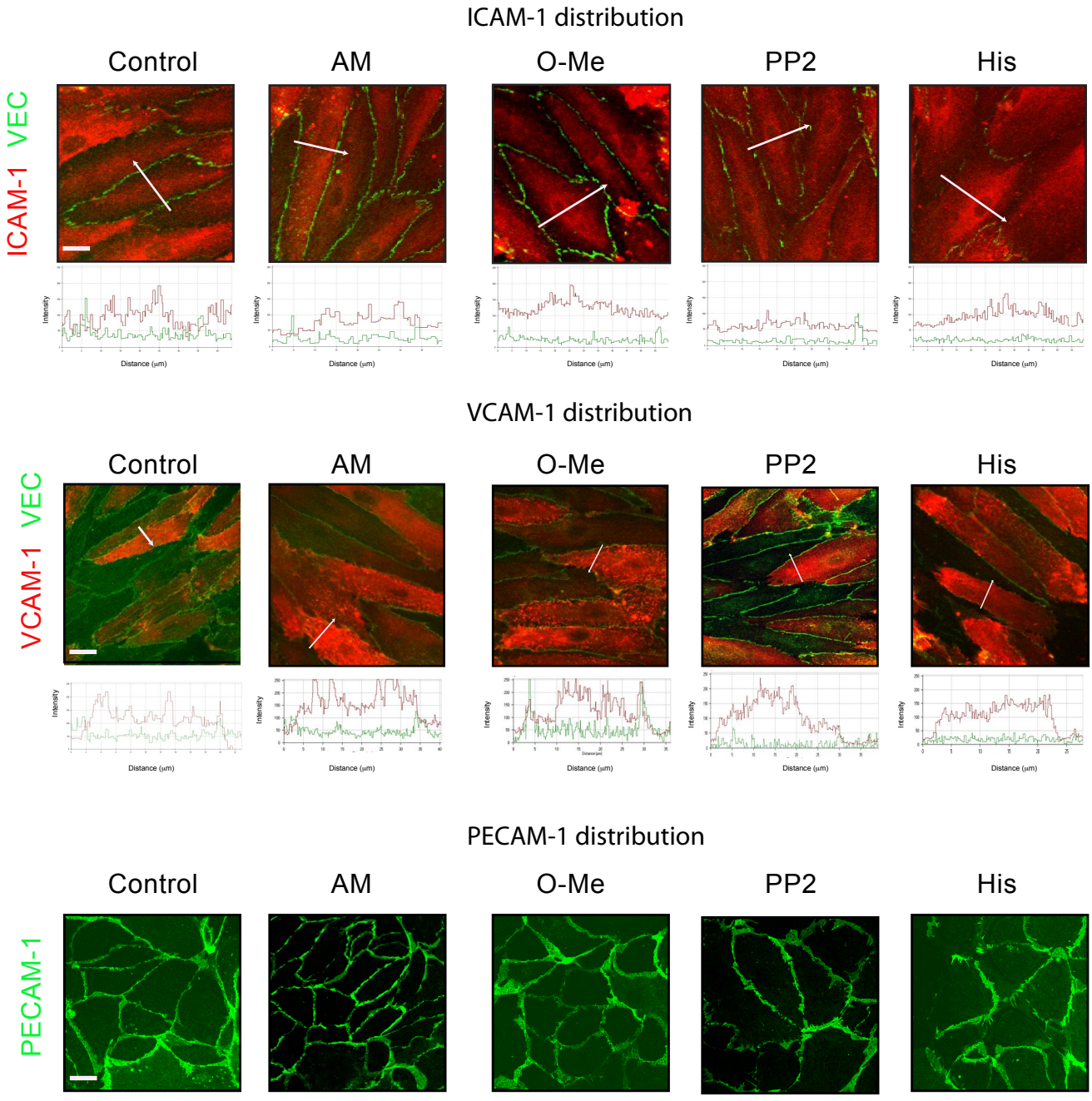
ICAM-1 distribution
Control
AM
O-Me
PP2
His
ICAM-1 VEC
VCAM-1 distribution
VCAM-1 VEC
PECAM-1 distribution
PECAM-1
Intensity
Distance (µm)

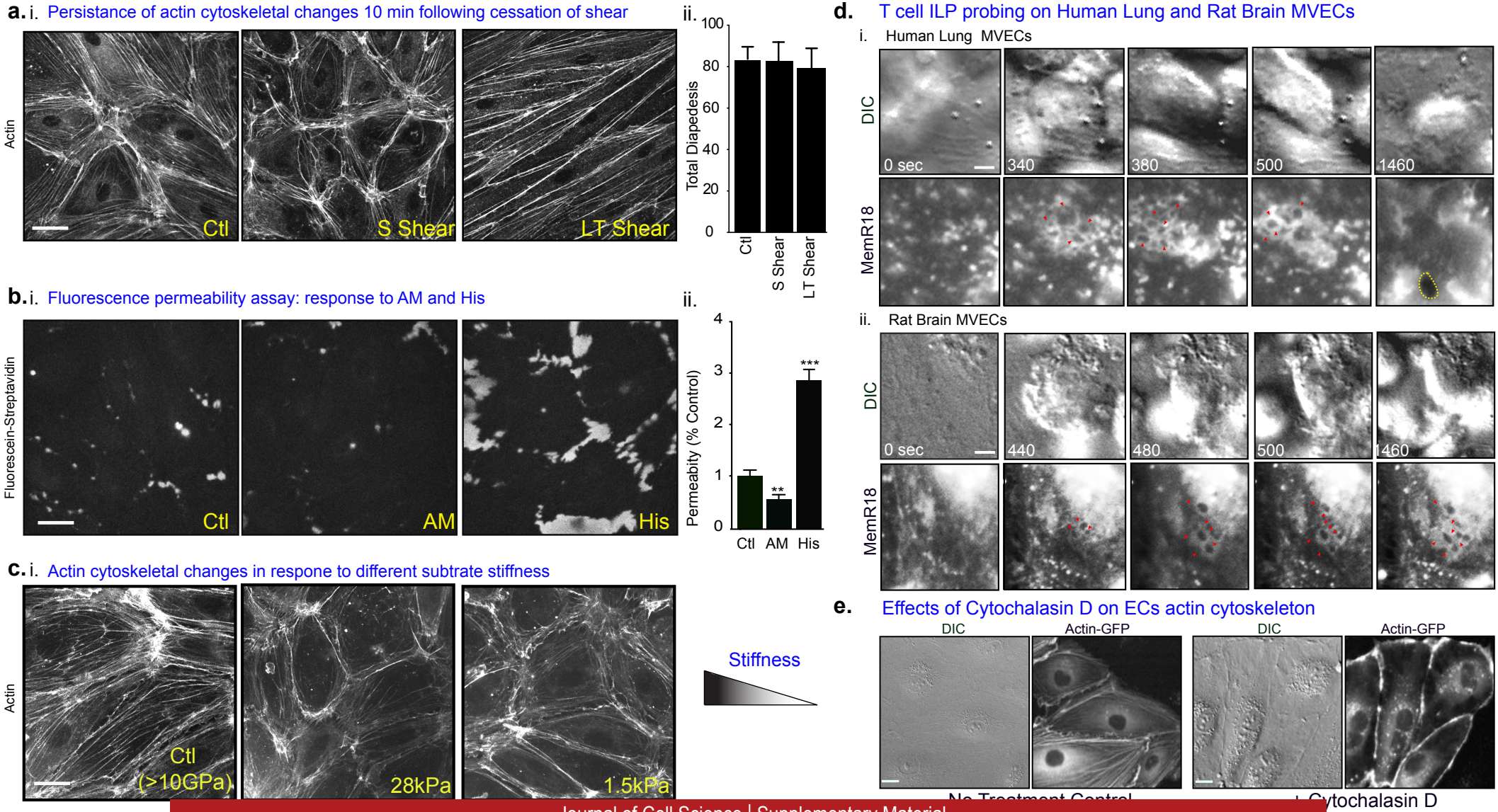
a. i. Persistance of actin cytoskeletal changes 10 min following cessation of shear
Actin
Ctl
S Shear
LT Shear
ii.
Total Diapedesis
100
80
60
40
20
0
Ctl
S Shear
LT Shear
b. i. Fluorescence permeability assay: response to AM and His
Fluorescein-Streptavidin
Ctl
AM
His
ii.
Permeabity (% Control)
4
3
2
1
0
**
***
Ctl
AM
His
c. i. Actin cytoskeletal changes in respone to different subtrate stiffness
Actin
Ctl
(>10GPa)
28kPa
1.5kPa
Stiffness
d. T cell ILP probing on Human Lung and Rat Brain MVECs
i. Human Lung MVECs
DIC
MemR18
0 sec
340
380
500
1460
ii. Rat Brain MVECs
DIC
MemR18
0 sec
440
480
500
1460
e. Effects of Cytochalasin D on ECs actin cytoskeleton
DIC
Actin-GFP
DIC
Actin-GFP
No Treatment Control
+ Cytochalasin D

Movie 1: Lymphocytes palpate the endothelium through invadosome-like protrusions (ILPs). Live-cell imaging of lymphocyte lateral migrating on MVEC transfected with memDsRed (magenta) and cytoplasmic-YFP (green). Parts I and II show a lymphocyte probing the endothelial cell junction or the cell body, respectively. Note the dynamic appearance and disappearance of circular rings of memDsRed fluorescence that correspond to cell surface invaginations ('podo-prints') reflective of invadosome-like protrusions (ILP) that are devoid of cytoplasmic-YFP. Images were acquired by time-lapse microscopy (Axiovert 200M; Carl Zeiss). Frames were taken every 30 s. See corresponding Fig.5c.

Movie 2: Frustrated ILPs probing on top of the nucleus. Live-cell imaging of a lymphocyte laterally migrating on MVEC transfected with mem-YFP (green). Note appearance of multiple 'non-productive/frustrated' podo-prints/ILP probing on top of the nucleus, followed by appearance of ILP and a transcellular breach point immediately adjacent to the nucleus. Images were acquired by time-lapse microscopy (Axiovert 200M; Carl Zeiss). Frames were taken every 30 s. See corresponding Fig.7b.

Movie 3: Lateral T cell migration and ILP probing across endothelial junctions without diapedesis. Live-cell imaging of lymphocytes laterally migrating on MVEC transfected with memDsRed (magenta) and actin-GFP (green). Note three separate lymphocytes migrating laterally and avidly probing over a junction, without initiating a diapedesis event. Images were acquired by time-lapse microscopy (Axiovert 200M; Carl Zeiss). Frames were taken every 30 s.

Movie 4: Frustrated ILPs probing and failed diapedesis in zones of dense F-actin. Live-cell imaging of lymphocytes laterally migrating on MVEC transfected with memDsRed (magenta) and actin-GFP (green). Note the frustrated and prolonged probing of a lymphocyte in an actin-dense area (lower left) without breaching of the endothelium. Another lymphocyte succeeds in creating a transcellular pore, but it is unable to sufficiently deform the actin meshwork to allow for migration, resulting in a failed diapedesis attempt. Images were acquired by time-lapse microscopy (Axiovert 200M; Carl Zeiss). Frames were taken every 30 s. See corresponding Fig.8ai.

Movie 5: Avid ILP-mediated distortion of F-actin networks during lateral migration and ultimate diapedesis. Live-cell imaging of a lymphocyte laterally migrating on MVEC transfected with memDsRed (magenta) and actin-GFP (green). Note that in the zone of modest F-actin density ILP probing causes appreciable bending and distortion of endothelial actin filaments, coupled to successful breaching of (and diapedesis across) the endothelium, when a zone of relatively reduced density of actin was reached. Images were acquired by time-lapse microscopy (Axiovert 200M; Carl Zeiss). Frames were taken every 30 s. See corresponding Fig.8b.

Movie 6: ILP-mediated endothelial cell breaching between two actin fiber to initiate diapedesis. Live-cell imaging of a lymphocyte laterally migrating on MVEC transfected with memDsRed (magenta) and actin-GFP (green). Note that the lymphocyte in a low F-actin density zone readily breaches and migrates across the endothelium by extending ILP between two actin filaments, which subsequently are 'bowed out' and distorted to accommodate completion of diapedesis. Images were acquired by time-lapse microscopy (Axiovert 200M; Carl Zeiss). Frames were taken every 30 s. See corresponding Fig.8aii.

Movie 7: Depletion of F-actin promotes avid transcellular diapedesis. Live-cell imaging of lymphocytes laterally migrating on MVEC that were transfected with memDsRed (magenta) and actin-GFP (green) and pre-treated with Cyto-chalasin D (200nM, 30 min) to deplete actin filaments. Note that actin filaments were profoundly lost within the endothelial cell body while a dense cortical actin ring was maintained at the junctions. In these conditions an extensive number of transcellular events can be seen, including several particular that were extremely close, but not migrating through the intact junction. See corresponding figure (Fig 8d) for post-fixation staining of VEC. Images were acquired by time-lapse microscopy (Axiovert 200M; Carl Zeiss). Frames were taken every 20 s.